Proceeding of the IEEE
International Conference on Robotics and Biomimetics (ROBIO)
Shenzhen, China, December 2013

Output Properties of Cellular Artificial Actuator

Shenshun. Ying, Shiming. Ji, Zhongfei. Wang and Zhun. Fan

Abstract—**This paper focuses on output properties of cellular artificial actuator. The actuator is built from small actuator cells with structural elasticity. These cells are connected together in series to form fibers, which are in turn connected in parallel to form the whole actuator. These cells are controlled to determine whether to be in a contracted, or ON, state or a relaxed, or OFF, state. Arranging the ON cells in different fibers of fixed topology gives different output properties. A model of actuator's stochastic behavior is firstly deduced. Then, the output properties of actuator in a fixed topology are exactly calculated. A SMA springs array with three rows and five columns are built to validate the algorithm. Effect of the SMA spring array with different activated cells on tensile is analyzed, and experiment data indicates there exists a serious coupling phenomenon within the SMA springs array. Finally, comparison of application of these two different analysis methods is presented.**

INTRODUCTION

Existing artificial muscle actuators (e.g. shape memory alloys, conducting polymers, pneumatic muscle actuator, and dielectric elastomers) possess characteristics such as high force-to-mass ratio, high efficiency, direct drive ability, high complicance and silent movement. These are promising for many applications including bionic device, aerospace, robot, medical device, and family health nursing assistant system. However, single artificial muscle actuator possesses limited force output and export displacement, and is difficult to meet many applications requiring great output power and multiple degrees of freedom. In consequent, study on drive method using a group of artificial muscle is becoming a concern.

For example, the Shadow Robot Company products a very dextrous 20-DOF pneumatic Bielefeld Shadow Hand. The hand comprises 24 joints, 20 of them are actively controllable. Each joint is actuated by an antagonistic pair of McKibben style pneumatic muscles. All muscles are packed densely in the lower forearm and the joints are actuated by means of tendons routed through the wrist and hand [1]. Hara induced polypyrrole-metal coil composite actuators as artificial muscle fibres. Even though one piece of Ppy-metal coil composite exhibits only 0.2 N force, a tiny 10-piece bundle can create 2.26 N (230 gf) force, and a bundle of 1600 pieces of PPy-metal coil composite was able to pull up 600 kg weight. More recently, Asada et al., have proposed assimilates the morphological structure of biological muscles. The artificial muscle actuator system has a cellular array structure. The cellular building blocks that can be actuated individually and that are connected in series and parallel to move specific points. The total displacement of the artificial muscle is determined by the integral of strains distributed over the individual building blocks in series. The output force is the summation of the force generation at the individual strands arranged in parallel. Asada et al studied systematically cellular actuators including a cellular design for a robotic hand with 12 SMA actuators [2, 3], design of PZT cellular actuators with power-law strain amplification [4] and its static lumped parameter model [5], dynamic analysis [6], and a broadcast-probability approach to the control of vast DOF cellular actuators [7]. Compared with single artificial muscle cell, a group of artificial muscles generated displacement and force can be easily tailored by adjusting the length and the number of artificial muscle cells, respectively [8, 9]. In addition, these output characteristics can be tailored to specific load conditions by activating the artificial muscle cells in a coordinated manner.

However, the output displacement and force of cellular actuator will be weakened due to various factors in reality, such as material characterization, layout structure, energy supply, and so on. In already mentioned Asada's group, a number of assumptions are made to keep things simple. For example, the net effect upon the output displacement and force is the summation and average of totally N_1N_2 PZT actuator. Where, N_1 and N_2 correspond to the number of the first and second rhombus units connected in series. In this section it is assumed that all mechanical structure is loss-less with no friction and energy dissipation within the structure [4]. This paper explores the influence of layout structure of cellular artificial muscles on output displacement and force. In Section II, the skeletal muscle structure is firstly explained, and a cellular artificial muscles actuator is then designed. In Section III-A, the idealized kinematics governing the motion of the cellular actuator are introduced. A model is then derived in Section II-B that considers the location influence on output displacement and force. Section III studies the output properties of a SMA springs array that has fixed topology in an experimental way. Section IV then discusses how to choose an optimal algorithm.

Manuscript received July 31, 2012. This work is partially supported by the Natural Science Foundation of Zhejiang Province under Grant Y1110953 and Scientific Research Fund of Zhejiang University of Technology under Grant 20100208

Shenshun. Ying is with Zhejiang University of Technology,Hangzhou, China. (86-0571-88320831; fax: 86-0571-88320372; e-mail: yss@zjut.edu.cn).

Shiming. Ji is with Zhejiang University of Technology, Hangzhou, China. (e-mail:jishiming@zjut.edu.cn).

Zhongfei Wang is with Zhejiang University of Technology, Hangzhou, China. (e-mail:wzfei@zjut.edu.cn).

Zhun. Fan is with Shantou University, Shantou, China. (e-mail:fanzhun@gmail.com).

978-1-4799-2744-9/13/$31.00 ©2013 IEEE

STRUCTURE OF CELLULAR ARTIFICIAL MUSCLE ACTUATOR

Fig.1 displays the skeletal muscle structure. Muscles comprise bundles of elastic fibers that contract to produce movement when stimulated by nerve impulses. Muscle cells are also known as muscle fibers that may reach lengths of up to 20 cm. They are divided into numerous units (sarcomeres) by transverse partitions called Z disks [10]. Within the sarcomere there is another regular arrangement of myofilaments, the thin actin and the thick myosin filaments. Each actin filament is anchored to the Z disk of a sarcomere, while the myosin filaments in the middle of the sarcomere protrude on both sides into the actin filaments (see Fig. 1). We know that muscle shortening corresponds to the sliding of thin (actin) filaments past thick (myosin) filaments. Most widely accepted mechanism for generation of force is the formation of connections between these filaments by cross-bridges. The strength of a muscle is determined by the length of muscle fibers [11].

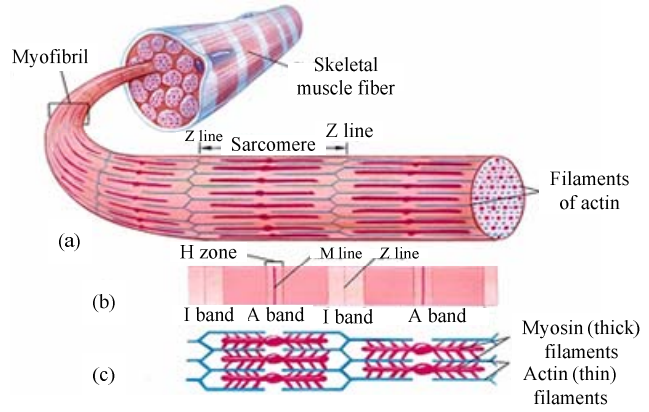

Fig.1. Skeletal muscle structure (a) skeletal muscle fiber; (b) myofibril; (c) sarcomere

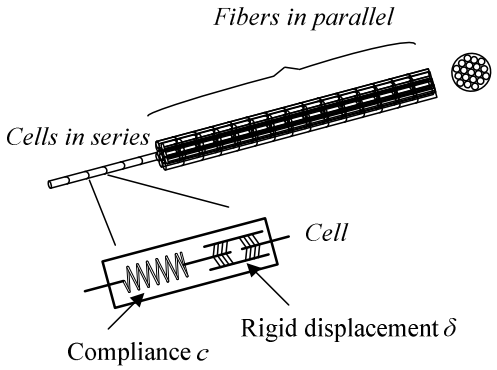

Fig.2. Cellular artificial muscle actuator inspired by the skeletal muscle structure[12]. Each cell corresponds to a sarcomere and is modeled as producing a displacement δ and a compliance c.

This paper designs a cellular muscle actuator inspired by the skeletal muscle structure. The cellular actuator architecture is broken down in a hierarchy of fibers and cells, shown in fig. 2. Cells are similar to sarcomere in skeletal muscle. These cells are connected together in series to form fibers, which are in turn connected in parallel to form the whole actuator.

OUTPUT PROPERTIES ANALYSIS

Model of the actuator's stochastic behavior

The actuator is composed of many small cells arranged in serial-parallel configuration. Each cell can be in a contracted, or ON, state or a relaxed, or OFF, state. Each cell is modeled as having a small rigid displacement δ in series with a small compliance c. The values of δ and c vary with the state of the cell,

$$\delta = \begin{cases} 0, & state = OFF \\ \eta, & state = ON \end{cases} \tag{1}$$

$$c = \begin{cases} c^{off}, & state = OFF \\ c^{on}, & state = ON \end{cases} \tag{2}$$

The displacement of the actuator can be predicted through the elastic averaging of each cell's displacement in this serial-parallel network. The actuator displacement and stiffness can be determined by a simple expression in terms of the total number of ON cells N^{on}. Because a fiber is composed of many compliant cells in series, the net displacement and compliance of each fiber is equal to the sum of the individual cell displacement and compliances within the chain. Namely,

$$\delta_j = \sum_{i=1}^{N_j} \delta i = \eta N_j^{on} + 0 N_j^{off} = \eta N_j^{on} \tag{3}$$

$$C_j = \sum_{i=1}^{N_j} c_i = N_j^{on} c^{on} + N_j^{off} c^{off} = N_j c^{off} + N_j^{on} (c^{on} - c^{off}) \tag{4}$$

Where, N_j^{on} is the number of ON cells within fiber j of the actuator. N_j^{off} is the number of OFF cells within fiber j of the actuator. The parallel combination of fibers to produce the actuator's net output y can be approximated as the average displacement of each fiber. For M fibers in parallel,

$$y \approx \eta N^{on} / M + F_d C \tag{5}$$

F_d is a disturbance force, and C is the net compliance of the actuator, which is assumed to be the average compliance of one chain divided by M.

$$C \approx \left[(N/M) c^{off} + \left(N^{on} / M \right) \left(c^{on} - c^{off} \right) \right] / M \tag{6}$$

The parallel combination of fibers to produce the actuator's net output F can be approximated as the summation force of each fiber.

$$F = \frac{y}{C} \approx \frac{\eta N^{on} / M + F_d C}{C}$$

$$= \frac{\eta N^{on}}{(N/M) c^{off} + \left(N^{on} / M \right) \left(c^{on} - c^{off} \right)} + F_d \tag{7}$$

The parse method

The parse method considers the effects of active location on output characteristics. For the above topology structure, cells in a fiber can be in contract state, and this motion

produces a linear displacement and tension. If one fiber is consistently shorter or longer than the others, the contribution of each fiber may not be uniform. Also, the compliance of each fiber can vary with the number of ON cells, so one fiber could potentially be stiffer or more compliant than the others. In consequence, not only the number of ON cells, but also the arrangement of the ON cells, can determine the output displacement and force.

Take M=3, N=27. If $N_1^{on}=1$ and $N^{on}=1$. There should be no bias in the arrangement of ON cells in certain fiber.

$c_1=8c^{off}+c^{on}$, $c_2=c_3=9c^{off}$, the value of net compliance of the actuator was equal to the values satisfying the expression.

$$C=\frac{1}{\frac{1}{c_1}+\frac{1}{c_2}+\frac{1}{c_3}}=\frac{1}{\frac{1}{8c^{off}+c^{on}}+\frac{2}{9c^{off}}} \tag{8}$$

The net output y and F are

$$y\approx\eta+F_dC \tag{9}$$

$$F=\frac{y}{C}\approx\frac{\eta+F_dC}{C}=\eta\left(\frac{1}{8c^{off}+c^{on}}+\frac{2}{9c^{off}}\right)+F_d \tag{10}$$

There are two kinds of combination when $N^{on}=2$. If $N_1^{on}=2$, namely, $c_1=7c^{off}+2c^{on}$, $c_2=c_3=9c^{off}$, we get

$$C=\frac{1}{\frac{1}{c_1}+\frac{1}{c_2}+\frac{1}{c_3}}=\frac{1}{\frac{1}{7c^{off}+2c^{on}}+\frac{2}{9c^{off}}} \tag{11}$$

The net output y and F are

$$y\approx 2\eta+F_dC \tag{12}$$

$$F=\frac{y}{C}\approx\frac{2\eta+F_dC}{C}$$

$$=2\eta\left(\frac{1}{7c^{off}+2c^{on}}+\frac{2}{9c^{off}}\right)+F_d \tag{13}$$

If $N_1^{on}=N_2^{on}=1$, namely, $c_1=c_2=8c^{off}+1c^{on}$, $c_3=9c^{off}$, we get

$$C=\frac{1}{\frac{1}{c_1}+\frac{1}{c_2}+\frac{1}{c_3}}=\frac{1}{\frac{2}{8c^{off}+c^{on}}+\frac{1}{9c^{off}}} \tag{14}$$

The net output y and F are

$$y\approx\eta+F_dC \tag{15}$$

$$F=\frac{y}{C}\approx\frac{\eta+F_dC}{C}$$

$$=\eta\left(\frac{2}{8c^{off}+c^{on}}+\frac{1}{9c^{off}}\right)+F_d \tag{16}$$

By that analog, we can deduce the various net output y and F as different values of N^{on}. Table I presents the number of assembly of cellular artificial muscle actuators in a fixed topology (M=3, N_1=N_2=N_3=9).

Without loss of generality, we need a formula to precisely calculate the number of output properties of cellular artificial muscle actuators in a fixed topology. This formula is about natural number split. This paper does not do further discussed.

TABLE I
RELATIONSHIP BETWEEN NUMBER OF ON CELLS AND OUTPUT PROPERTIES
(M=3, N_1=N_2=N_3=9)

Number of ON cells	0	1	2	3	4	5
Number of output properties	1	1	2	3	4	5
Number of ON cells		…	$n\times m$ -3	$n\times m$ -2	$n\times m$ -1	$n\times m$
Number of output properties	7	…	3	2	1	1

EXPERIMENT

To validate the validity of the algorithm above, the paper analyzed the output properties of a cellular artificial actuator that has fixed topology. Fig.3 is the topology diagram of the SMA springs array, it has five rows and three columns. M1-M5 respectively represent amount of activated SMA springs in each row. The cellular artificial actuator using the same specifications of Ni-Ti SMA springs. Each SMA spring has 20 mm for length, 0.62 mm for wire diameter and 4.2 mm for nominal diameter. Nylon cord having a length of 40 mm is used to connect SMA springs. Fig.4 shows the prototype of the SMA springs array and attached platform.

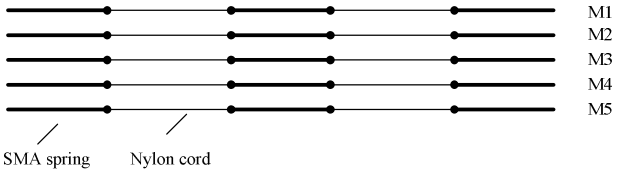

Fig.3. Topology diagram of a 5×3 SMA springs array

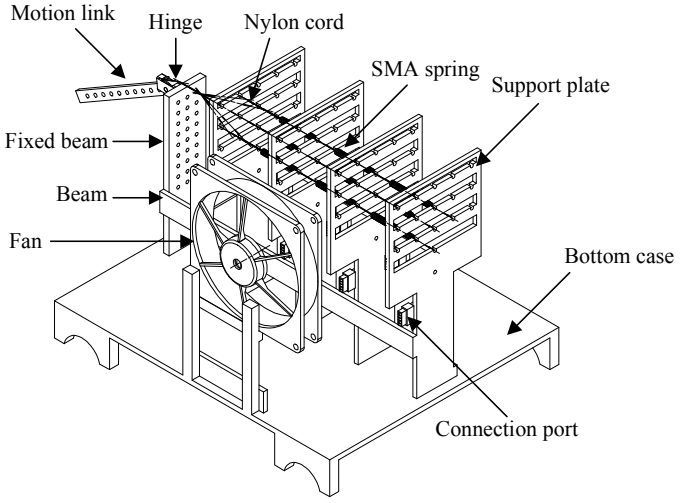

Fig.4. Prototype of SMA springs array and attached platform

Fig.5 shows the experiment setup, which includes the

following parts: SMA springs array and attached platform, control apparatus, personal computer, and test system, which includes ondoscope, LMS SCADAIII-305 frontend system, laser displacement sensor and force transducers. SMA spring will contract back to initial length under no-load state when 2.5 amp current through circuit for 5 seconds, while it is extended manually to two times of initial length in advance. Control apparatus determines the on-off of the circuit. Signals from the force transducer are transmitted into LMS SCADAS III frontend, and further sampled and calculated.

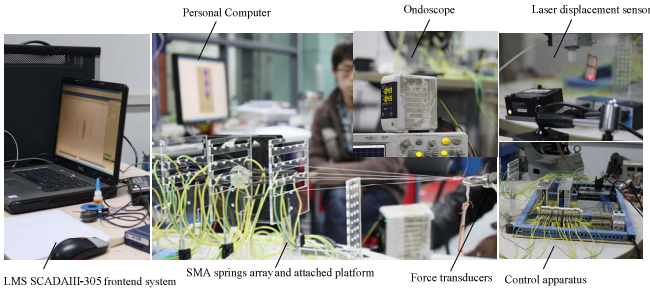

Fig.5. Experiment setup

TABLE II
SCHEME THAT HAS DIFFERENT ACTIVATED SMA SPRING

Order	Sum of M1-M5	M1	M2	M3	M4	M5
run 1	0	0	0	0	0	0
run 2	1	1	0	0	0	0
run 3	2	1	1	0	0	0
run 4	2	2	0	0	0	0
run 5	3	1	1	1	0	0
run…	…	…	…	…	…	…
run 54	14	2	3	3	3	3
run 55	15	3	3	3	3	3

Fig. 6 represents the effect of the SMA springs array with different activated cells on tensile. As shown here, the tensile of SMA spring array changes from maximum 2.3 N to minimum -3.3 N, and the maximum difference is equal to 5.6 N. The tensile of the SMA springs array attenuates in the course of the array contract, which can be divided into four stages. In the case of run 37, the peak tensile of SMA springs array is roughly 0 N in the first stage, roughly 2.3 N in the second stage, roughly 1 N in the third stage, and returns to roughly 0 N in the fourth stage. In the case of run 55, the peak tensile of the SMA springs array is roughly 2.5 N, when all the 15 SMA springs are activated. As shown in fig.6, there is no insignificant difference in the tensile of SMA springs array between the eight runs. This shows big difference exists between the experimental data and the theoretical result. This indicates that there exists a serious coupling phenomenon within the SMA springs array, which seriously weakens the tensile of the SMA springs array. However, this mechanism and suppression method may not be that simple, and more research is needed.

Fig.6 shows the attenuation of tensile oscillation of the SMA spring array. The test system may relate to the negative tensile of SMA spring array: In order to eliminate the influence of inertia force of the force transducer, a tray that moves at a constant velocity is added to the test system, which forms a typical second-order oscillation systems. The solution for this situation is to tune the velocity of the force transducer.

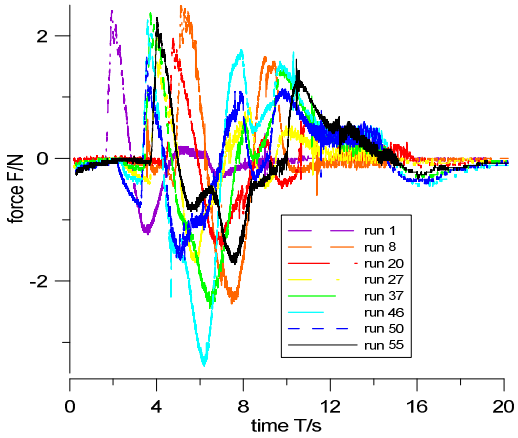

Fig.6. Tensile of SMA springs array. Where, numbers of activated cells respectively equal to run1、 run 8、 run20、run27、run37、run 46、run 50、run 55, and that are given in table II.

DISCUSSION

The model of the actuator' stochastic behavior can be implemented using a relevant stochastic optimal control laws[12]. The actuator is embedded a small decision maker within each cell that causes the cell to switch randomly between ON and OFF states. Because the actuator displacement is a summation of each cell's randomly determined displacement, the central limit theorem guarantees that the variance of the actuator response will quickly become small as the number of cells becomes large, yielding an almost deterministic response. But the deterministic response cannot be yielded when the number of cells is small, as mentioned in section II-B, the compliance of each fiber can vary with the number of ON cells, in consequence, the actuator have different output properties. In that case, model of the actuator' analytic behavior should be used. In addition, the coupling effect on tensile of SMA springs array is uppermost.

REFERENCES

[1] F. Rothling, et al. Platform portable anthropomorphic grasping with the bielefeld 20-dof shadow and 9-dof tum hand. in Proceedings of IEEE/RSJ International Conference on Intelligent Robots and Systems. 2007.

[2] K.J. Cho, J. Rosemarin, and H. Asada. Design of vast DOF artificial muscle actuators with a cellular array structure and its application to a five-fingered robotic hand. in International Conference on Robotics and Automation. 2006. Orlando, Florida: IEEE.

[3] K.J. Cho, J. Rosmarin, and H. Asada. SBC Hand: A Lightweight Robotic Hand with an SMA actuator Array implementing C-segmentation. in International Conference on Robotics and Automation. 2007. Roma, Italy: IEEE.

[4] J. Ueda, T. Secord, and H.H. Asada. Design of PZT cellular actuators with power-law strain amplification. in International Conference on Intelligent Robots and Systems. 2007. San Diego, CA, USA: IEEE.

[5] J. Ueda, T. Secord, and H.H. Asada. Static lumped parameter model for nested PZT cellular actuators with exponential strain amplification mechanisms. in International Conference on Robotics and Automation. 2008. Pasadena, CA, USA: IEEE.
[6] T.W. Secord, J. Ueda, and H.H. Asada. Dynamic analysis of a high-bandwidth, large-strain, pzt cellular muscle actuator with layered strain amplification. in International Conference on Robotics and Automation. 2008. Pasadena, CA, USA: IEEE.
[7] J. Ueda, L. Odhnar, and H. Asada. A broadcast-probability approach to the control of vast DOF cellular actuators. in International Conference on Robotics and Automation. 2006. Orlando, Florida: IEEE.
[8] K.J.D. Laurentis, et al. Optimal Design of Shape Memory Alloy Wire Bundle Actuators. in Proceedings of IEEE International Conference on Robotics and Automation. 2002. Washington,USA.
[9] K. Suzumori, et al., Development of Artificial Muscles Using a Bundle of McKibben Muscle Fibers. Nippon Kikai Gakkai Robotikusu, Mekatoronikusu Koenkai Koen Ronbunshu (CD-ROM), 2005. 2005.
[10] A. Faller and M. Schuenke, The Humman Body : An Introduction to Structure and Function. 2004, New York: Georg Thieme Verlag.
[11] Atherton, A., et al., Illustrated Guide to the Human Body: Skeletal and Muscular Systmens, ed. L. Bender, et al. 2005, New York: the diagram group.
[12] L. Odhner, J. Ueda, and H.H. Asada. Stochastic optimal control laws for cellular artificial muscles. in International Conference on Robotics and Automation. 2007. Roma, Italy: IEEE.